http://dx.doi.org/10.5012/bkcs.2014.35.12.3542

End-to-end Structural Restriction of α-Synuclein and Its Influence on Amyloid Fibril Formation

Chul-Suk Hong, Jae Hyung Park, Young-Jun Choe, and Seung R. Paik*

*School of Chemical and Biological Engineering, Institute of Chemical Processes, College of Engineering, Seoul National University, Seoul 151-744, Korea. *E-mail: srpaik@snu.ac.kr*
Received July 21, 2014, Accepted August 19, 2014

Relationship between molecular freedom of amyloidogenic protein and its self-assembly into amyloid fibrils has been evaluated with α-synuclein, an intrinsically unfolded protein related to Parkinson's disease, by restricting its structural plasticity through an end-to-end disulfide bond formation between two newly introduced cysteine residues on the N- and C-termini. Although the resulting circular form of α-synuclein exhibited an impaired fibrillation propensity, the restriction did not completely block the protein's interactive core since co-incubation with wild-type α-synuclein dramatically facilitated the fibrillation by producing distinctive forms of amyloid fibrils. The suppressed fibrillation propensity was instantly restored as the structural restriction was unleashed with β-mercaptoethanol. Conformational flexibility of the accreting amyloidogenic protein to pre-existing seeds has been demonstrated to be critical for fibrillar extension process by exerting structural adjustment to a complementary structure for the assembly.

Key Words : Amyloid fibril, Molecular freedom, Self-assembly, Structural restriction, α-Synuclein

Introduction

Amyloids are insoluble protein aggregates with highly ordered structure resulted from specific self-assembly of soluble proteins. Amyloids can be classified into two types; 'disease-associated amyloids' and 'biologically functional amyloids'.[1,2] The disease-associated amyloids are commonly found in various neurodegenerative disorders such as Alzheimer's, Parkinson's, and Huntington's diseases.[3-5] Although a cause-and-effect relationship between amyloids and the cellular degeneration remains elusive, amyloids and/or their induction process per se have been considered to be pathologically crucial to the diseases.[5,6] In bacteria, the biologically functional amyloids play critical roles on their survival by involving in biofilm formation of *E. coli* (curli fibrils) and aerial hyphae formation of *S. coelicolor* (chaplain amyloid fibrils).[7,8] Despite their functional diversity, amyloids share some common physicochemical features.[5,9] They form unbranched fibrils with a thickness of about 10 nm, which can be extended to a few micrometers in length.[10] These fibrils have been demonstrated to exhibit fibrillar polymorphism as observed with the straight and curly forms produced from a single protein of α-synuclein depending on how they were prepared.[11] Fibrillar backbone consists of the common hydrogen-bonded β-sheets stacking perpendicular to the fibrillar axis to form cross-β sheet conformation, which provides molecular basis for the rigidity of amyloid fibrils ranging from 2 to 14 GPa (Young's modulus).[12,13] The structural regularity gives rise to an apple-green birefringence as Congo red molecules are regularly intercalated.[14] Amyloid fibrils have been recognized as a promising material for biotechnological applications since they exhibit not only mechanical robustness[12,13] but also physical and chemical stability against heat, pH, and solvent treatment.[15] These protein nanofibrils could be utilized in multi-dimensional formats. One-dimensional conductive protein nanofibrils were prepared by entrapping gold-nanoparticles in the peapod type fibrils.[16] The protein fibrils were also fabricated into two-dimensional film[17] or three-dimensional hydrogels,[11,18] which could be used for drug delivery system and tissue engineering. In addition, the nanofibrils could serve for a raw substance to produced hybrid materials with organic[19] or inorganic products including graphene[20] and nanoparticles,[21] whose improved functionality allows them to be widely employed in nanobiotechnology.

Recent investigation by Simone *et al.*[22] indicated that highly dynamic region of a fungal protein, hydrophobin, affected its self-aggregation property, in which the flexible structural element was demonstrated to lower the amyloid forming propensity. On the contrary, however, unfolded state of amyloidogenic proteins/peptides was suggested to be crucial for the fibrillation process.[23] The flexible region of these proteins/peptides has contributed to conformational rearrangement essential for their oligomerization and subsequent fibrillation. To clarify whether the flexibility and thus conformational freedom of amyloidogenic proteins are critical for their assembly into the fibrils, we have investigated amyloidogenesis of an intrinsically unstructured protein of α-synuclein by restricting its structural freedom. α-Synuclein is a pathological protein comprised of 140 amino acids,[24] and its progressive accumulation into amyloid fibrils is found in the Lewy bodies of α-synucleinopathies including Parkinson's disease, dementia with Lewy bodies[25] and multiple system atrophy.[26] Primary structure of α-synuclein can be divided into three regions:[27] (i) an amphipathic N-terminal region (residues 1-60) suggested to interact with

lipid membrane, (ii) a hydrophobic central region (residues 61-95) containing the non-Aβ component (NAC) segment, and (iii) a highly acidic C-terminal stretch (residues 96-140). The N-terminus adopts α-helical conformation when it interacts with lipid membranes.[28] The NAC region is indispensable for the fibrillation since the lack of a large part of this region affected the aggregation property considerably.[29] The C-terminal acidic region was found to be highly flexible even within the amyloid fibrils as evaluated with solid-state NMR.[30]

In this study, molecular flexibility of α-synuclein has been restricted by stapling the protein end-to-end between N- and C-termini, and its influence on the amyloid fibril formation has been observed. This structural restriction approach, therefore, could improve our understanding toward not only criticalness of the molecular freedom for self-assembly but also another debated issue on the long-range contact between N- and C-termini of α-synuclein which has been suggested to diminish its fibrillation potential by hiding a core region of the self-assembly.[31,32] This long-range contact, however, was also demonstrated to expose a part of the hydrophobic NAC segment.[33] The current investigation, therefore, unveils the assembly mechanism of α-synuclein in terms of its molecular freedom and the long-range intramolecular contact, which may eventually contribute to the development of diagnostic and therapeutic strategies toward the α-synucleinopathies as well as producing amyloid-based biocompatible nanomaterials.[11,16]

Experimental

Expression and Purification of Recombinant α-Synuclein. For site-directed mutagenesis, the Val3Cys and Ala140Cys double point mutations were introduced into human α-synuclein gene within pRK172 by using the QuickChange method (Stratagene). Created mutant plasmids were transformed into *E. coli* BL21(DE3). After induction with 0.5 mM IPTG, cells were pelleted and resuspended with 20 mM Tris-Cl, pH 7.5, containing 0.1 M NaCl. Cell lysate was boiled for 15 min and centrifuged at 30,000 x g for 15 min. After filtration, the supernatant was applied onto DEAE-anion exchange column pre-equilibrated with 20 mM Tris-Cl, pH 7.5, containing 1 mM dithiothreitol (DTT). α-Synuclein was eluted *via* salt gradient with 0.4 M NaCl. Fractions containing α-synuclein were pooled and concentrated, which was then further purified with S-200 gel filtration chromatography by using 20 mM 2-(*N*-morpholino)-ethanesulfonic acid (Mes), pH 6.5, containing 1 mM DTT. The purified mutant proteins containing the cysteines were oxidized with diamide, a thiol-oxidizing agent, at room temperature for 5 min. Then they were loaded onto the S-200 gel filtration column to remove any oligomeric species and residual diamide. The oxidized proteins were purified in 20 mM Mes, pH 6.5, and stored at −80 °C until used. Wild type α-synuclein was also purified with the same procedure described above.

High-Performance Liquid Chromatography (HPLC). Purity of the oxidized protein and its relationship with wild-type α-synuclein were evaluated with reversed-phase HPLC equipped with C4 column (250 × 4.6 mm; Vydac, Hesperia, CA). After injection of the sample containing the protein (4 nmol) in 20 mM Mes, pH 6.5, the chromatography was performed with a linear gradient between 0.1% trifluoroacetic acid (TFA) and 80% acetonitrile in 0.1% TFA at a flow rate of 1.0 mL/min at room temperature.

Thioflavin-T Binding Assay. To monitor the fibrillation kinetics of α-synuclein, thioflavin-T (Th-T) binding fluorescence assay was performed with a luminescence spectrophotometer (LS-55, Perkin-Elmer, Waltham, MA). Aliquot (20 μL) of the sample containing α-synuclein at 70 μM was mixed with Th-T (25 μM) in 180 μL of 50 mM glycine, pH 8.5. Following 5 min of incubation under dark at room temperature, the Th-T binding fluorescence was monitored at 482 nm with an excitation at 450 nm.

8-Anilinonaphthalene-1-sulfonic acid (ANS) Binding Assay. Samples were prepared by mixing α-synuclein monomer and ANS in 20 mM Mes, pH 6.5. Final concentration of the protein and ANS were 17.5 μM and 25 μM, respectively. After incubated for 5 min at room temperature, their fluorescence spectra were measured with a luminescence spectrophotometer (LS-55, Perkin-Elmer, Waltham, MA). The spectra were obtained *via* accumulation of three scans between 400 nm and 650 nm with a scan speed of 200 nm/min upon an excitation at 350 nm.

Circular Dichroism (CD) Spectroscopy. Transition of the secondary structures of α-synuclein was monitored with CD spectroscopy. After dilution of the protein (0.5 mg/mL) with 20 mM Mes, pH 6.5, by five-fold, the CD spectra were monitored between 195 and 250 nm with a scan speed of 20 nm/min in a quartz cuvette of 1.0 mm-path length. All the spectra were obtained as an average of five separate scans.

Transmission Electron Microscope (TEM). The final protein aggregates were visualized with TEM (JEM1010, JEOL, Japan). An aliquot of the sample was dropped onto a carbon-coated copper grid (200 mesh) and air-dried. Then, 20 μL of 2% uranyl acetate (Electron Microscopy Sciences, Hatfield, PA) was treated for negative staining of the amyloid fibrils. The staining step was performed in a darkroom to prevent uranyl acetate from degradation.

Results

Preparation of the Restricted Circular Form α-Synuclein. Disulfide bond formation between cysteine residues was employed to restrict the structural freedom of α-synuclein. Since wild-type α-synuclein (WTαS) does not have its own cysteine residue, the N- and C-terminal residues of valine at 3 and alanine at 140 were replaced with cysteines *via* site-directed mutagenesis (Fig. 1A). The cysteine double mutant protein was purified in the presence of 1 mM DTT throughout all the procedure described in Materials and Methods except the final step of gel filtration chromatography. Diamide as a thiol-oxidizing agent was then added to specifically oxidize the newly introduced cysteine residues.

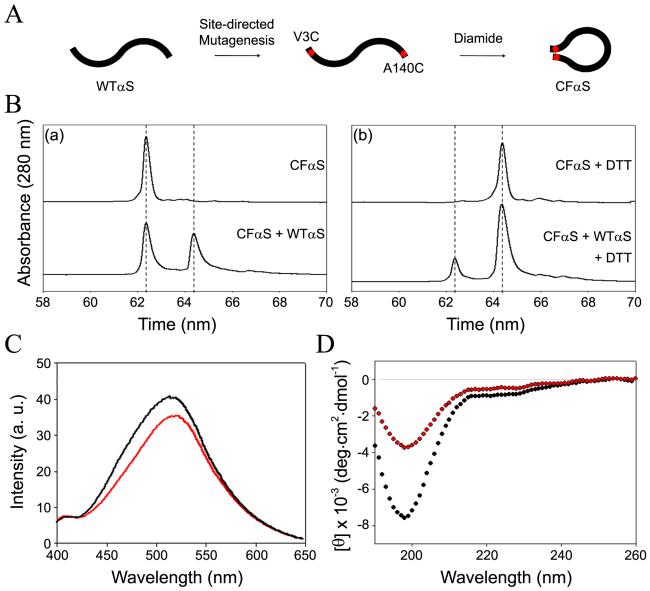

Figure 1. Preparation and characterization of CFαS. A. Schematic illustration of preparing CFαS *via* site-directed mutagenesis and disulfide-bond formation using diamide. B. HPLC chromatograms of CFαS and WTαS. Elution of CFαS and WTαS from C4 reversed-phase column following pre-incubation in the absence (a) or presence (b) of DTT. C. ANS binding fluorescence spectra of CFαS (red) and WTαS (black) with an excitation at 350 nm. D. CD spectra of CFαS (red) and WTαS (black).

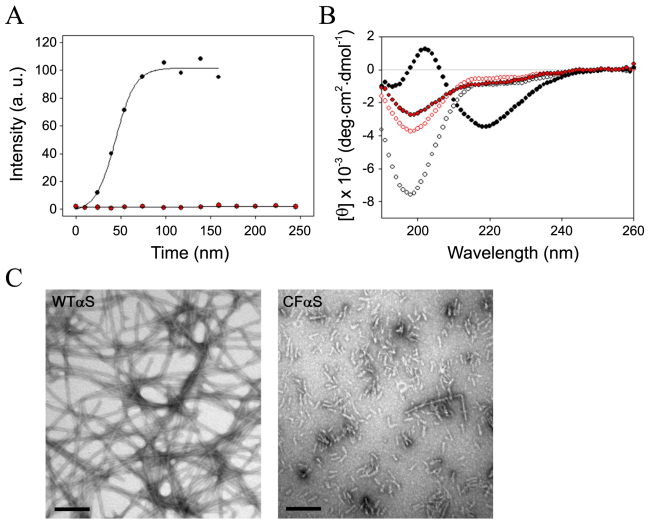

Figure 2. Amyloid fibrillation kinetics of CFαS and WTαS. A. Thioflavin-T binding fluorescence was monitored as the fibrillation proceeded for either WTαS (black) or CFαS (red). B. CD spectra of either CFαS (red) or WTαS (black) before (open dot) and after (closed dot) the fibrillation incubation. C. TEM images of the WTαS fibrils after 159 h of incubation and the CFαS aggregates after 400 h (Scale bars, 200 nm).

Diamide was originally developed to oxidize glutathione, and it has been used since then for sulfhydryl group-specific oxidation steps.[34] The resulting double mutant protein, therefore, could form either intra- or inter-molecular disulfide bond, which leads to circular or oligomeric α-synuclein, respectively. The restricted circular form α-synuclein (CFαS) was separated from the oligomers with Sepharose S-200 gel-filtration chromatography. Purity of the isolated CFαS was confirmed by a reversed-phase HPLC with C4 column as the protein was eluted in a symmetrical peak at 62.3 min; CFαS was eluted earlier than WTαS emerging at 64.3 min (Fig. 1B-(a)). With DTT pre-treatment, the elution of CFαS was delayed to the time point of 64.3 min, indistinguishable from the WTαS elution; the conversion of CFαS to WTαS was also confirmed in the presence of DTT as the WTαS peak was augmented while the CFαS peak decreased (Fig. 1B-(b)). Taken together, CFαS was shown to be less hydrophobic than WTαS in addition to the fact that the CFαS was readily prepared from WTαS. ANS binding study also indicated that CFαS exhibited the reduced ANS binding fluorescence from that of WTαS (Fig. 1C). Upon the CFαS formation, therefore, a hydrophobic region(s) appeared to be concealed from the ANS access. Circular dichroism (CD) spectra clearly revealed that CFαS formation produced a local structure which decreased the random structure of WTαS by raising the minimum ellipticity at 196 nm to a significant level (Fig. 1D). All the data illustrated that the end-to-end restriction of α-synuclein has decreased its molecular flexibility by producing local ordering and thus concealing a hydrophobic region(s).

Fibrillation Characteristics of CFαS. Self-assembly of CFαS into amyloid fibrils was evaluated with thioflavin-T (Th-T) binding fluorescence, which was compared with that of WTαS. Even after more than 10 days of incubation at 37 °C with agitation, CFαS was not able to increase the fluorescence while WTαS showed a typical sigmoidal aggregation kinetics reaching the stationary phase within 100 h (Fig. 2A). The CD analyses also indicated that local structure of CFαS was slightly affected upon the incubation while WTαS exhibited a typical drastic transition from random to β-sheet structures (Fig. 2B). As confirmed with TEM image, WTαS indeed turned into the amyloid fibrils as evidenced with the kinetics and CD data (Fig. 2C). Intriguingly, however, CFαS also showed rather short and thin fibrillar aggregates although its fibrillation kinetics and CD data did not indicate any fibril formation (Fig. 2C). In other words, CFαS did not completely lose its potential for self-assembly although its fibrillation propensity was clearly affected by the structural restriction.

In order to clarify whether CFαS still has the interactive core available for self-assembly, the restricted CFαS was co-incubated with WTαS at various ratios under shaking condition at 37 °C. In the absence of CFαS, WTαS at 35 μM exhibited the fibrillation kinetics reaching the stationary phase within 50 h (Fig. 3A), which resulted in the amyloid fibrils as confirmed with CD and TEM analyses (Fig. 3B and C). Surprisingly, the amyloid fibrillation was dramatically increased as CFαS was included at various proportions to the 35 μM WTαS (Fig. 3A) whereas CFαS alone at 35 μM hardly produced any fibrils to a significant level even after 217 h of prolonged incubation (Fig. 3A). The increase in amyloid fibril formation was also confirmed with CD and TEM analyses (Fig. 3B and C). CD analysis indicated that

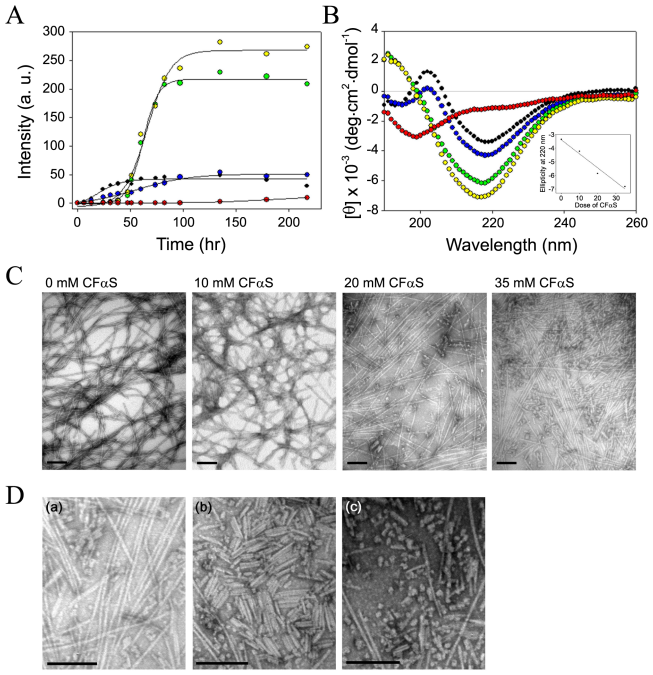

Figure 3. Co-incubation between CFαS and WTαS. A. Fibrillation kinetics monitored with thioflavin-T binding fluorescence for 35 μM WTαS with CFαS at 0 μM (black), 10 μM (blue), 20 μM (green), and 35 μM (yellow). Red dots represent CFαS at 35μM in the absence of WTαS. B. CD spectra of the corresponding final aggregates obtained in the fibrillation kinetics of A after 217 h. Inset shows a linear relationship between the ellipticity at 220 nm and the amount of CFαS added. C. TEM images of the final aggregates obtained in the presence of various concentrations of CFαS. D. TEM images of the three-different types of fibrils obtained from the WTαS and CFαS mixture at a 1:1 molar ratio after 217 h of incubation (Scale bars, 200 nm).

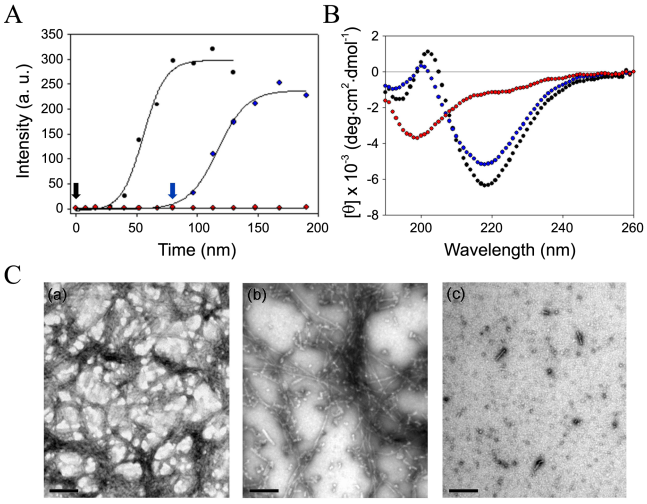

Figure 4. Unleashing the structural restriction of CFαS and its influence on the fibrillation. A. Fibrillation kinetics monitored with thioflavin-T binding fluorescence for CFαS in the presence and absence of the β-ME treatment at the points indicated with the arrows. CD spectra B and TEM images C of the final aggregates obtained in the fibrillation kinetics of CFαS A in the absence (red dots; C-(a)) or presence of β-ME treated from the beginning (black dots; C-(b)) and in the middle (blue dots; C-(c)) of the fibrillation at the end of incubation (Scale bars, 200 nm).

the β-sheet content evaluated with the minimum ellipticity at 217 nm increased as the CFαS level was raised (Fig. 3B and inset). The spectrum also confirmed that CFαS alone failed to transform into the β-sheet structure. When examined with TEM, the amyloid fibrils became noticeably thinner as CFαS was included. At the highest CFαS concentration in particular, the fibrils comprised of three distinctive types in terms of their length (Fig. 3D). Even though the fibrils existed in a mixed population, emergence of the morphologically distinctive fibrils from the short fibrils obtained only with CFαS and the thick fibrils made of WTαS alone indicated that CFαS has apparently participated in the fibrillation of WTαS. In other words, the interactive core of CFαS for the amyloid fibril formation did not appear to be completely concealed although its potential for self-assembly has been obviously affected.

Restoration of the Fibrillation Propensity of CFαS. To delineate whether the structural restriction was responsible for the suppressed fibrillation propensity of CFαS, the amyloid fibrillation was carried out with CFαS whose structural restraint was relieved in the middle of the kinetics. Three separate samples containing 70 μM CFαS were incubated in a 37 °C shaking incubator. The structural restriction was unleashed by reducing the disulfide bond with β-mercaptoethanol (β-ME). When the CFαS incubation was performed with β-ME from the beginning, the amyloid fibrillation occurred by showing the typical sigmoidal kinetics with a definitive lag phase (Fig. 4A). The resulting fibrils showed the β-sheet structure on CD spectrum and their morphology was revealed with TEM (Fig. 4B and 4C-(a)). They were rather thick fibrils similar to those obtained with WTαS. When β-ME was added to another CFαS after 80 h of incubation, the fibrillation responded instantly without any lag phase (Fig. 4A). The fibrillar assembly was proceeded for another 80 h to be completed, which resulted in the β-sheet structure formation (Fig. 4A and B). Interestingly, the resulting fibrils appeared mostly well-extended in the presence of small spheres (Fig. 4C-(b)), in which the middle-sized and short fibrils previously found in the aggregates of the WTαS and CFαS mixture were missing (Fig. 3D). In the absence of β-ME, CFαS was not able to form the mature fibrils (Fig. 4C-(c)). The data clearly suggest that the fibrillation propensity has been successfully restored upon the release of structural restriction. In addition, the lack of lag phase and the presence of mostly extended fibrils observed during the restoration process may indicate that the structural restriction would have interfered with the fibrillar extension process.

Discussion

Structural flexibility of α-synuclein as an intrinsically unfolded protein (IUP) has been suspected to play an important role on the amyloid fibril formation especially for either ligand-dependent or seed-dependent fibrillar polymorphism.[23] Current investigation of the end-to-end restriction

of α-synuclein was planned to establish a relationship between structural freedom of an amyloidogenic protein and its propensity to be self-assembled into amyloid fibrils. Our trial to restrict the conformational freedom with the disulfide bond formation between N- and C-termini of α-synuclein, however, could bury the interactive core essential for the self-assembly. In fact, the long-range contact of α-synuclein was suggested to shield the interactive hydrophobic NAC segment.[31,32] Our data indicated that the restriction actually led to a local structure formation and thus reduced exposure of hydrophobic region(s). This artificially introduced long-range contact, however, was not able to completely block the interactive core because CFαS produced either the homogeneous short fibrils by themselves or the mixed population of amyloid fibrils in the presence of WTαS. The results also suggest that the suppressed structural freedom appeared to limit the fibrillar extension since the short fibrils obtained with CFαS became elongated instantly without any delay as the disulfide-mediated restriction was unleashed with β-ME. Taken together, molecular freedom would be crucial for the amyloidogenesis as the amyloidogenic protein approaches and exhibits conformational adjustment to pre-existing seeds which have also been demonstrated to contain the flexible C-terminal region of α-synuclein with solid-state NMR.[30] In conclusion, current investigation suggests that structural adjustment of both accreting α-synuclein and the accommodating seeds would be essential for the formation of mature and fully extended amyloid fibrils, reflecting that general induced-fit process has been involved in the amyloid fibril formation.

Acknowledgments. This work was supported by a grant of the Korean Health Technology R&D Project, Ministry of Health & Welfare, Republic of Korea (A120870-1201-0000100).

References

1. Hammer, N. D.; Wang, X.; McGuffie, B. A.; Chapman, M. R. *J. Alzheimers Dis.* **2008**, *13*(4), 407-419.
2. Fowler, D. M.; Koulov, A. V.; Balch, W. E.; Kelly, J. W. *Trends Biochem. Sci.* **2007**, *32*(5), 217-224.
3. Irvine, G. B.; El-Agnaf, O. M.; Shankar, G. M.; Walsh, D. M. *Mol. Med.* **2008**, *14*(7-8), 451.
4. Ross, C. A.; Poirier, M. A. *Nature Med.* **2004**, *10*, S10-S17.
5. Chiti, F.; Dobson, C. M. *Annu. Rev. Biochem.* **2006**, *75*, 333-366.
6. Hardy, J.; Selkoe, D. J. *Science* **2002**, *297*(5580), 353-356.
7. Chapman, M. R.; Robinson, L. S.; Pinkner, J. S.; Roth, R.; Heuser, J.; Hammar, M.; Normark, S.; Hultgren, S. J. *Science* **2002**, *295*(5556), 851-855.
8. Claessen, D.; Rink, R.; de Jong, W.; Siebring, J.; de Vreugd, P.; Boersma, F. H.; Dijkhuizen, L.; Wösten, H. A. *Genes Dev.* **2003**, *17*(14), 1714-1726.
9. Nelson, R.; Sawaya, M. R.; Balbirnie, M.; Madsen, A. Ø.; Riekel, C.; Grothe, R.; Eisenberg, D. *Nature* **2005**, *435*(7043), 773-778.
10. Corrigan, A. M.; Müller, C.; Krebs, M. R. *J. Am. Chem. Soc.* **2006**, *128*(46), 14740-14741.
11. Bhak, G.; Lee, S.; Park, J. W.; Cho, S.; Paik, S. R. *Biomaterials* **2010**, *31*(23), 5986-5995.
12. Knowles, T. P.; Fitzpatrick, A. W.; Meehan, S.; Mott, H. R.; Vendruscolo, M.; Dobson, C. M.; Welland, M. E. *Science* **2007**, *318*(5858), 1900-1903.
13. Smith, J. F.; Knowles, T. P.; Dobson, C. M.; MacPhee, C. E.; Welland, M. E. *Proc. Natl. Acad. Sci. USA* **2006**, *103*(43), 15806-15811.
14. Puchtler, H.; Sweat, F.; Levine, M. *J. Histochem. Cytochem.* **1962**, *10*(3), 355-364.
15. Ridgley, D. M.; Barone, J. R. *ACS nano* **2013**, *7*(2), 1006-1015.
16. Lee, D.; Choe, Y. J.; Choi, Y. S.; Bhak, G.; Lee, J.; Paik, S. R. *Angew. Chem. Int. Ed.* **2011**, *50*(6), 1332-1337.
17. Knowles, T. P.; Oppenheim, T. W.; Buell, A. K.; Chirgadze, D. Y.; Welland, M. E. *Nat. Nanotechnol.* **2010**, *5*(3), 204-207.
18. Chun, J.; Bhak, G.; Lee, S. G.; Lee, J. H.; Lee, D.; Char, K.; Paik, S. R. *Biomacromolecules* **2012**, *13*(9), 2731-2738.
19. Choi, Y. S.; Kim, J.; Bhak, G.; Lee, D.; Paik, S. R. *Angew. Chem. Int. Ed.* **2011**, *123*(27), 6194-6198.
20. Li, C.; Adamcik, J.; Mezzenga, R. *Nat. Nanotechnol.* **2012**, *7*(7), 421-427.
21. Scheibel, T.; Parthasarathy, R.; Sawicki, G.; Lin, X. M.; Jaeger, H.; Lindquist, S. L. *Proc. Natl. Acad. Sci. USA* **2003**, *100*(8), 4527-4532.
22. De Simone, A.; Kitchen, C.; Kwan, A. H.; Sunde, M.; Dobson, C. M.; Frenkel, D. *Proc. Natl. Acad. Sci. USA* **2012**, *109*(18), 6951-6956.
23. Uversky, V. N.; Fink, A. L. *Biochim. Biophys. Acta* **2004**, *1698*(2), 131-153.
24. Uéda, K.; Fukushima, H.; Masliah, E.; Xia, Y.; Iwai, A.; Yoshimoto, M.; Otero, D. A.; Kondo, J.; Ihara, Y.; Saitoh, T. *Proc. Natl. Acad. Sci. USA* **1993**, *90*(23), 11282-11286.
25. Arima, K.; Uéda, K.; Sunohara, N.; Hirai, S.; Izumiyama, Y.; Tonozuka-Uehara, H.; Kawai, M. *Brain Res.* **1998**, *808*(1), 93-100.
26. Arima, K.; Uéda, K.; Sunohara, N.; Arakawa, K.; Hirai, S.; Nakamura, M.; Tonozuka-Uehara, H.; Kawai, M. *Acta Neuropathol.* **1998**, *96*(5), 439-444.
27. Rasia, R. M.; Bertoncini, C. W.; Marsh, D.; Hoyer, W.; Cherny, D.; Zweckstetter, M.; Griesinger, C.; Jovin, T. M.; Fernández, C. O. *Proc. Natl. Acad. Sci. USA* **2005**, *102*(12), 4294-4299.
28. Davidson, W. S.; Jonas, A.; Clayton, D. F.; George, J. M. *J. Biol. Chem.* **1998**, *273*(16), 9443-9449.
29. Giasson, B. I.; Murray, I. V.; Trojanowski, J. Q.; Lee, V. M. Y. *J. Biol. Chem.* **2001**, *276*(4), 2380-2386.
30. Heise, H.; Hoyer, W.; Becker, S.; Andronesi, O. C.; Riedel, D.; Baldus, M. *Proc. Natl. Acad. Sci. USA* **2005**, *102*(44), 15871-15876.
31. Dedmon, M. M.; Lindorff-Larsen, K.; Christodoulou, J.; Vendruscolo, M.; Dobson, C. M. *J. Am. Chem. Soc.* **2005**, *127*(2), 476-477.
32. Bertoncini, C. W.; Jung, Y. S.; Fernandez, C. O.; Hoyer, W.; Griesinger, C.; Jovin, T. M.; Zweckstetter, M. *Proc. Natl. Acad. Sci. USA* **2005**, *102*(5), 1430-1435.
33. Ullman, O.; Fisher, C. K.; Stultz, C. M. *J. Am. Chem. Soc.* **2011**, *133*(48), 19536-19546.
34. Kosower, N. S.; Kosower, E. M.; Wertheim, B.; Correa, W. S. *Biochem. Biophys. Res. Commun.* **1969**, *37*(4), 593-596.